Thermal scanning probe lithography for nanoscale magnetic domain switching

Zhengming Wu [1], Tero S. Kulmala [1], Edoardo Albisetti [2], Daniela Petti [2], Riccardo Bertacco [2] and Elisa Riedo [3]
[1] Heidelberg Instruments Nano AG, Zurich, Switzerland
[2] Dipartimento di Fisica, Politecnico di Milano, Milan, Italy
[3] New York University Tandon School of Engineering, NY, United States

Thermal Probe

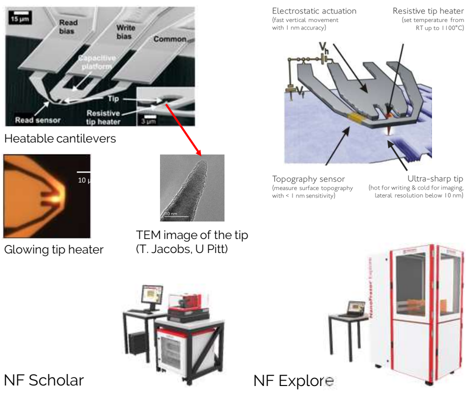

Closed-Loop Lithography

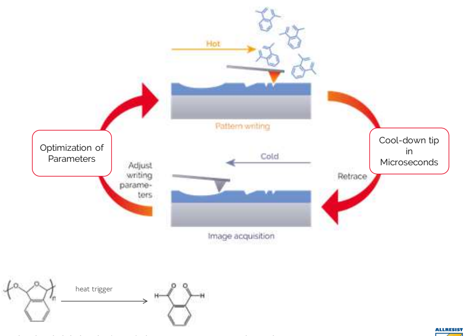

Polyphtalaldehyde (PPA) decomposes upon heat impact
PPA commercially available as Phoenix81 from AllResist, Germany

Pattern transfer

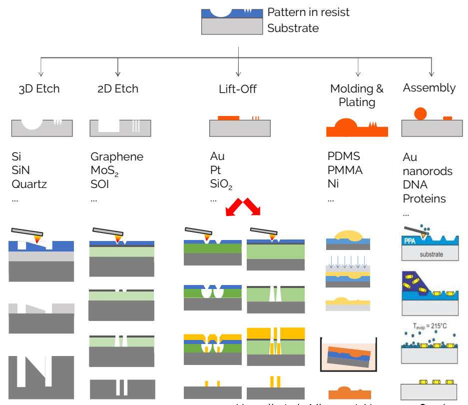

Howell et al., *Microsyst. Nanoeng.*, **6**:21 (2020).

Thermally assisted magnetic scanning probe lithography [1-6]

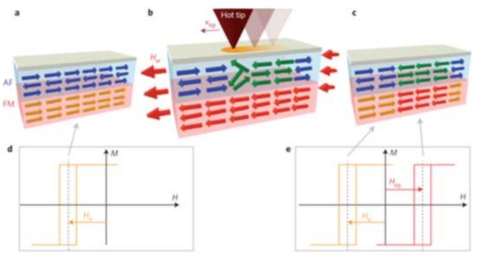

Magnetic patterning via tam-SPL. **a)** The initialization state where the ferromagnetic (FM) layer (yellow arrows) is uniformly pinned in one direction by the exchange interaction with the antiferromagnetic (AF) layer (blue arrows). **b)** Sweeping a heated SPM tip on the sample surface in the presence of an external magnetic field H_w resets the exchange bias direction according to the underlying CoFeB spins (red arrows). **c)** The magnetic domain configuration in the ferromagnet is stabilized by the local exchange bias without presence of H_w. **d,e)** Magnetic hysteresis loops before (**d**) and after (**e**) patterning. H_e and H_{ep} indicate the opposite shift in the loops due to the exchange bias in the non-patterned and patterned areas, respectively. [2]

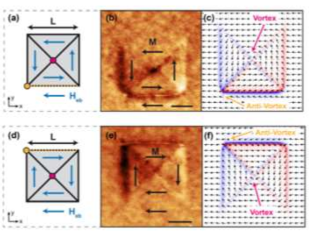

Stabilization of vortex-antivortex pairs. **a)** and **d)** Schematics showing the configuration of the exchange bias patterned via tam-SPL in the IrMn/CoFeB system. The blue arrow indicates the direction of the patterned exchange bias. L is the lateral size of the pattern. The pink (orange) circles mark the position of the vortex core (antivortex). The orange dotted line marks the 180° Neel domain wall. **b)** and **e)** MFM images of the patterned structure for counter clockwise and clockwise orientations. The direction of the magnetization is indicated by the black arrows. The scale bar is 2 µm. **c)** and **f)** Corresponding simulated micromagnetic configuration showing the location of the vortex and antivortex and the direction of the spins; the red/blue color marks div (**M**), which is related to the measured MFM contrast. [3]

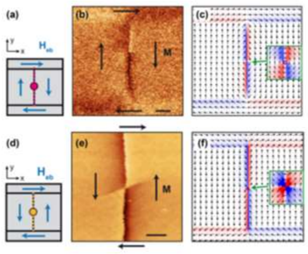

Stabilization of antivortex and vortex Bloch lines within patterned domain walls. **a,d)** Sketches showing the geometry and direction of the patterned exchange bias for stabilizing vortex and antivortex Bloch lines, respectively. The vortex (antivortex) Bloch line is indicated by the pink (yellow) circle, and the corresponding 180° Neel domain wall is marked by the dashed line. **b,e)** MFM images of the patterned structures for the vortex and antivortex Bloch lines, respectively. The scale bar is 3 µm. **c,f)** Simulated micromagnetic configuration for the vortex and antivortex Bloch lines, respectively. [3]

Engineered spin textures and nanomagnonic circuits

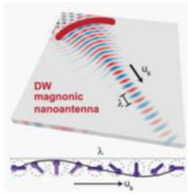

Simulation of spatially shaped spin-wave wavefronts generated by a curved nanoantenna. u_k marks the spin-wave propagation direction. The precession of the spins along a single spin-wave wavelength λ is shown at the bottom. [6]

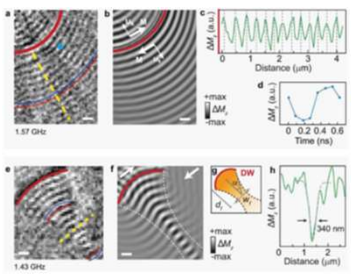

Spin-wave wavefront engineering. **a)** Experimental STXM image and **b)** micromagnetic simulation of the directional emission of convex spin-wave wavefronts by a curved domain wall (red line). Wavefronts are indicated by thin red and blue lines. **c,d)** Spatial and temporal profiles extracted from the yellow dashed line and blue dot in **a)**. Strong spin-wave intensity is measured after more than 15 periods of propagation. **e)** Experimental image and **f)** simulation of the emission and focusing of spin-wave beams with concave wavefronts. **g)** Diffractive-optics analogy of spin-wave focusing by a magnonic nanoantenna with angular aperture 2α. **h)** Spatial profile of the spin-wave amplitude along the dashed line in **e)**. At the beam waist, located 2.5 µm away from the emitter, spin waves are localized in a region comparable to the spin-wave wavelength ~340 nm. Scale bars: 500 nm. [6]

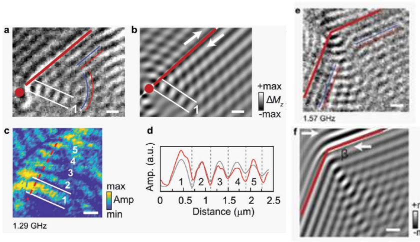

Generation of multi-beam interference patterns. **a)** Experimental STXM image and **b)** simulations of the interference from radial wavefronts emitted by a vortex (red dot) and planar wavefronts (red line) emitted from a straight domain wall. **c)** Constructive and destructive interference fringes are visible as alternated minima (blue) and maxima (yellow). The first interference maximum is indicated by white lines in **a–c)**. **d)** Experimental (red) and simulation (gray) spatial profile of the spin-wave amplitude extracted from the red dashed line in **c)**; **e)** Experimental and **f)** simulated interference pattern generated by the spin-wave wavefronts emitted by two angled domain wall nanoantennas. The two linear wavefronts are indicated by thin red and blue lines. The white arrows indicate the equilibrium magnetization direction of the top layer. Scale bars: 500 nm. The microscopy was carried out at the Swiss Light Source at Paul Scherrer Institute, Switzerland. [6]

Direct Laser Sublimation for large area patterning

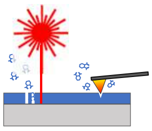

- Mix & match; no new processing steps needed
- λ = 405 nm
- Resolution ~1 µm → faster throughput for writing e.g. contact pads
- Seamless stitching with t-SPL written patterns

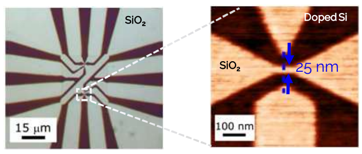

A single-electron transistor fabricated by the mix & match approach. [7] The contacts were patterned by a laser and the high-resolution features by t-SPL.

Nanofluidics for Brownian motors

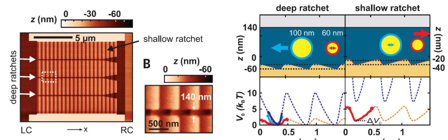

Nano PPA ratchets for sorting 60-nm and 100-nm Au nanoparticles. **Left:** Device topography made by t-SPL. **Right:** Top: device schematics, roughly to scale with experimental conditions. Bottom: corresponding measured (solid) and modelled (dashed) static energies. [8]

No damage to sample

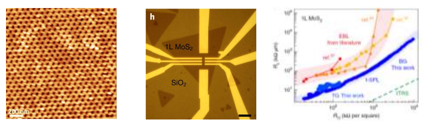

Electron or ion beam lithography can damage the sample by introducing vacancies or unwanted charges into it. T-SPL avoids such damage as it uses heat for removing the thermal resist locally. **Left**: This approach allows studying the intrinsic properties of sensitive nanomaterials such as graphene nano-dot arrays; **Center**: Device with MoS2 flakes and metal electrodes for testing; **Right**: Comparison of contact resistance Rc of electrodes patterned via t-SPL as a function of the sheet resistance RS to values for EBL-fabricated devices found in literature. [9].

Broad choice of substrates

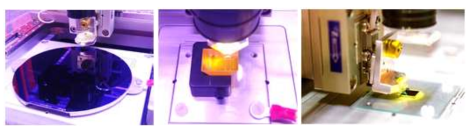

As NanoFrazor lithography works in ambient environment, outgassing of materials is not an issue. Almost any substrate can be patterned: conducting, insulating, magnetic, etc.

References

[1] E. Albisetti et al., Comm. Phys., 1 (56) **2018.**.
[2] E. Albisetti et al., *Nat. Nanotechnol. 11 (545)* **2016.**
[3] E. Albisetti et al., *Appl. Phys. Lett. 113 (162401)* **2018.**
[4] E. Albisetti et al., *AIP Adv. 7 (055601)* **2017.**
[5] E. Albisetti et al., *J. Magn. Magn. Mater. 400 (230)* **2016.**
[6] E. Albisetti et al., Adv. Mater. (1906439) **2020.**
[7] Rawlings et al., *Nanotechnology*, 29 (505302) **2018.**
[8] Skaug et al., Science, 359 (1505) **2018.**
[9] Zheng *et al.*, *Nat. Electron.*, 2 (17) **2019.**

The research leading to these results received funded by the European Union's Horizon 2020 research and innovation programme under grant agreements 705326 (SWING), 730872 (CALIPSOplus), 948225 (B3YOND).

Thermal scanning probe lithography

Thermal Probe

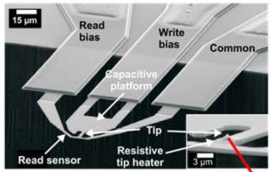

Heatable cantilevers

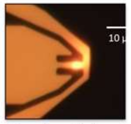
Glowing tip heater

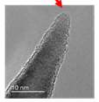
TEM image of the tip
(T. Jacobs, U Pitt)

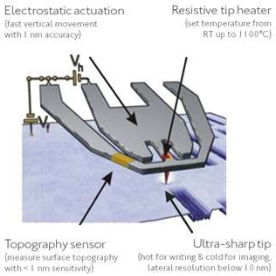

NF Scholar

NF Explore

Closed-Loop Lithography

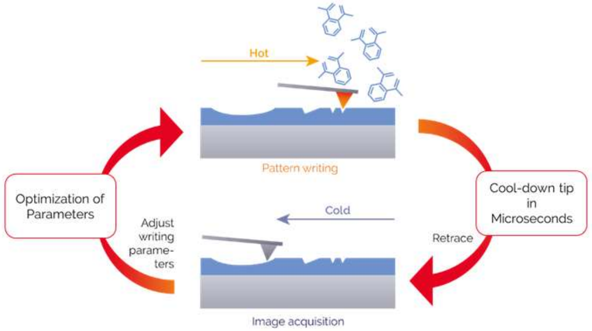

Polyphtalaldehyde (PPA) decomposes upon heat impact
PPA commercially available as Phoenix81 from AllResist, Germany

Pattern transfer

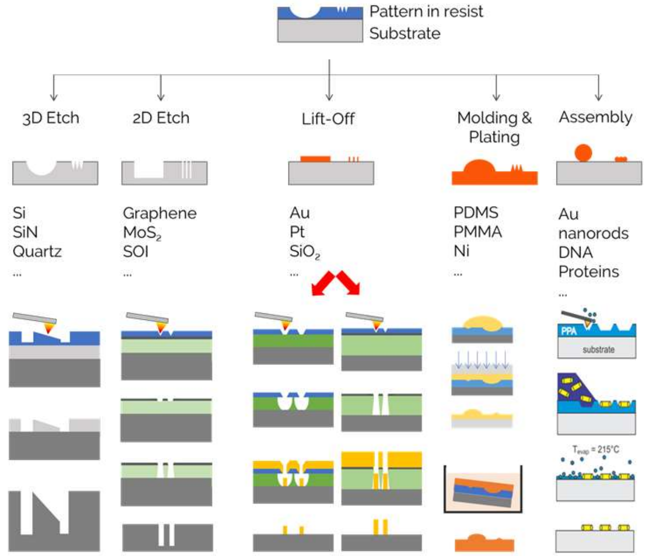

Howell et al., *Microsyst. Nanoeng.*, 6:21 (2020).

Nanofluidics for Brownian motors

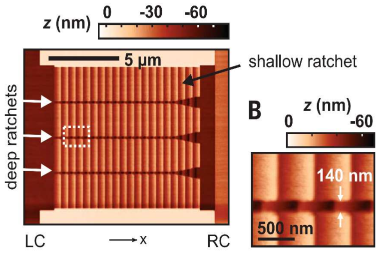

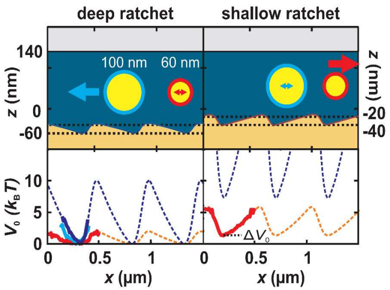

No damages to sample

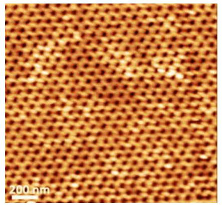

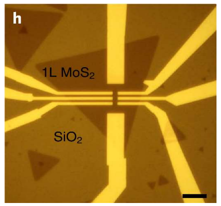

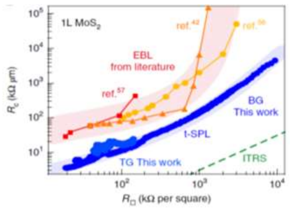

Thermally assisted magnetic scanning probe lithography [1-6]

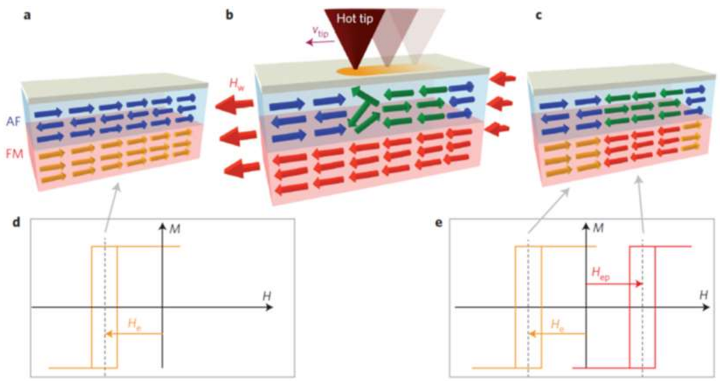

Magnetic patterning via tam-SPL. **a)** The initialization state where the ferromagnetic (FM) layer (yellow arrows) is uniformly pinned in one direction by the exchange interaction with the antiferromagnetic (AF) layer (blue arrows). **b)** Sweeping a heated SPM tip on the sample surface in the presence of an external magnetic field H_w resets the exchange bias direction according to the underlying CoFeB spins (red arrows). **c)** The magnetic domain configuration in the ferromagnet is stabilized by the local exchange bias without presence of H_w. **d,e)** Magnetic hysteresis loops before **(d)** and after **(e)** patterning. H_e and H_{ep} indicate the opposite shift in the loops due to the exchange bias in the non-patterned and patterned areas, respectively. [2]

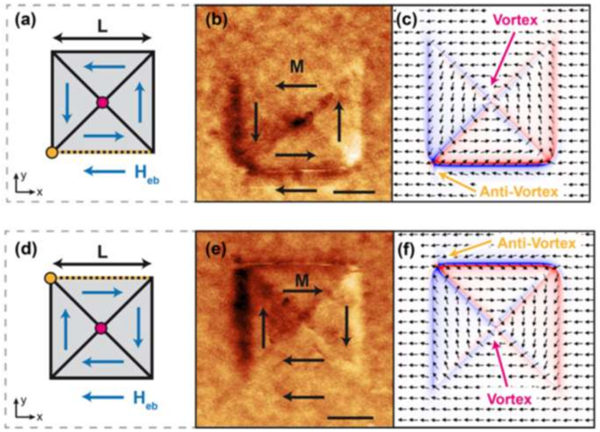

Stabilization of vortex-antivortex pairs. **a)** and **d)** Schematics showing the configuration of the exchange bias patterned via tam-SPL in the IrMn/CoFeB system. The blue arrow indicates the direction of the patterned exchange bias. **L** is the lateral size of the pattern. The pink (orange) circles mark the position of the vortex core (antivortex). The orange dotted line marks the 180° Neel domain wall. **b)** and **e)** MFM images of the patterned structure for counter clockwise and clockwise orientations. The direction of the magnetization is indicated by the black arrows. The scale bar is 2 µm. **c)** and **f)** Corresponding simulated micromagnetic configuration showing the location of the vortex and antivortex and the direction of the spins; the red/blue color marks div (**M**), which is related to the measured MFM contrast. [3]

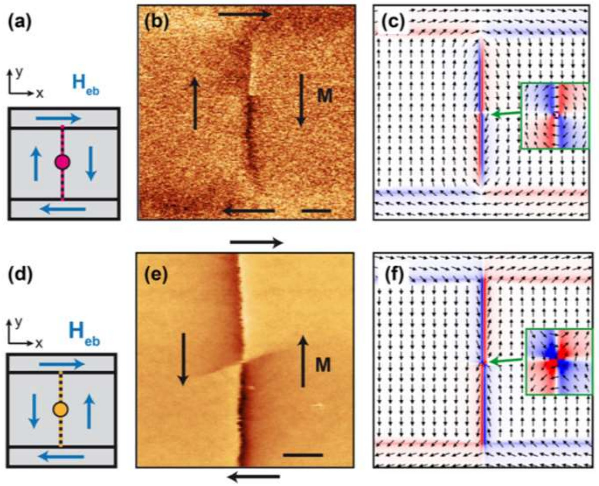

Stabilization of antivortex and vortex Bloch lines within patterned domain walls. **a,d)** Sketches showing the geometry and direction of the patterned exchange bias for stabilizing vortex and antivortex Bloch lines, respectively. The vortex (antivortex) Bloch line is indicated by the pink (yellow) circle, and the corresponding 180° Neel domain wall is marked by the dashed line. **b,e)** MFM images of the patterned structures for the vortex and antivortex Bloch lines, respectively. The scale bar is 3 µm. **c,f)** Simulated micromagnetic configuration for the vortex and antivortex Bloch lines, respectively. [3]

Engineered spin textures and nanomagnonic circuits

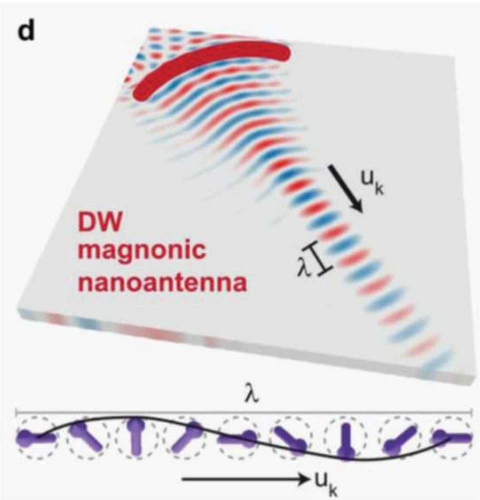

Simulation of spatially shaped spin-wave wavefronts generated by a curved nanoantenna. u_k marks the spin-wave propagation direction. The precession of the spins along a single spin-wave wavelength λ is shown at the bottom. [6]

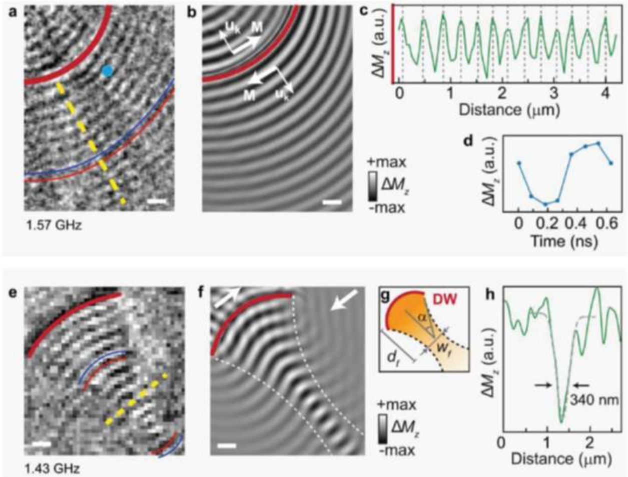

Spin-wave wavefront engineering. **a)** Experimental STXM image and **b)** micromagnetic simulation of the directional emission of convex spin-wave wavefronts by a curved domain wall (red line). Wavefronts are indicated by thin red and blue lines. **c,d)** Spatial and temporal profiles extracted from the yellow dashed line and blue dot in **a)**. Strong spin-wave intensity is measured after more than 15 periods of propagation. **e)** Experimental image and **f)** simulation of the emission and focusing of spin-wave beams with concave wavefronts. **g)** Diffractive-optics analogy of spin-wave focusing by a magnonic nanoantenna with angular aperture 2α. **h)** Spatial profile of the spin-wave amplitude along the dashed line in **e)**. At the beam waist, located 2.5 µm away from the emitter, spin waves are localized in a region comparable to the spin-wave wavelength ~340 nm. Scale bars: 500 nm. [6]

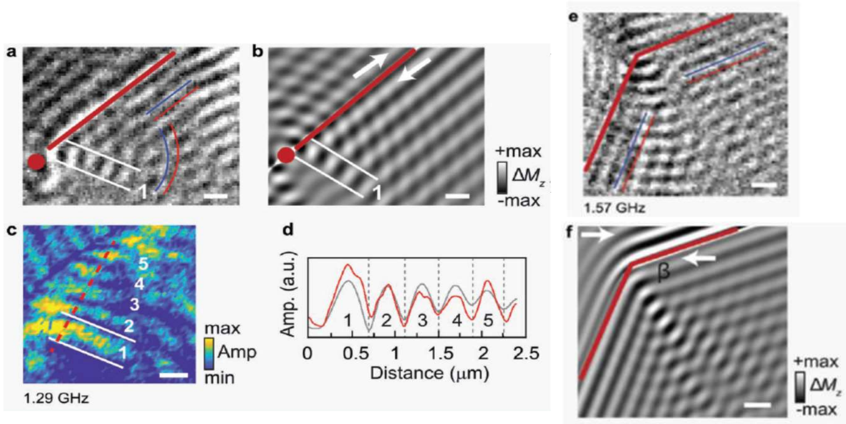

Generation of multi-beam interference patterns. **a)** Experimental STXM image and **b)** simulations of the interference from radial wavefronts emitted by a vortex (red dot) and planar wavefronts (red line) emitted from a straight domain wall. **c)** Constructive and destructive interference fringes are visible as alternated minima (blue) and maxima (yellow). The first interference maximum is indicated by white lines in **a–c)**. **d)** Experimental (red) and simulation (gray) spatial profile of the spin-wave amplitude extracted from the red dashed line in **c)**; **e)** Experimental and **f)** simulated interference pattern generated by the spin-wave wavefronts emitted by two angled domain wall nanoantennas. The two linear wavefronts are indicated by thin red and blue lines. The white arrows indicate the equilibrium magnetization direction of the top layer. Scale bars: 500 nm. The microscopy was carried out at the Swiss Light Source at Paul Scherrer Institute, Switzerland. [6]

NanoFrazor System

Direct Laser Sublimation for large area patterning

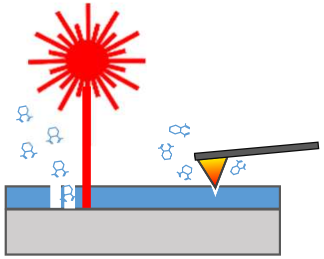

- Mix & match; no new processing steps needed
- λ = 405 nm
- Resolution ~1 µm → faster throughput for writing e.g. contact pads
- Seamless stitching with t-SPL written patterns

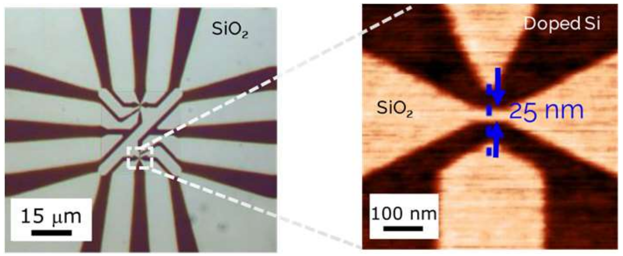

Decapede extension

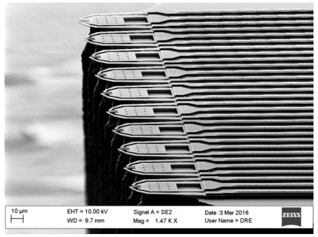

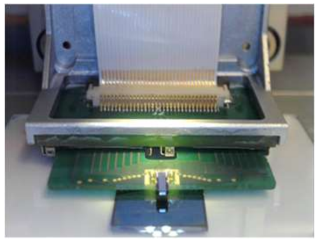

Broad choice of substrates

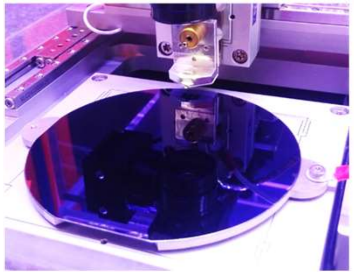

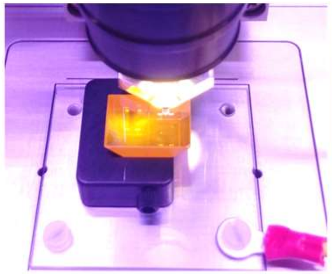

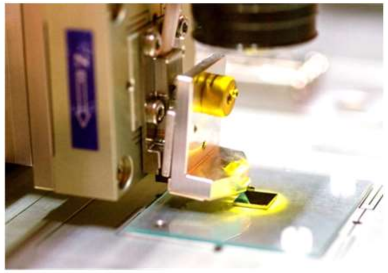

As NanoFrazor lithography works in ambient environment, outgassing of materials is not an issue. Almost any substrate can be patterned: conducting, insulating, magnetic, etc.

Stitching for large-area patterning

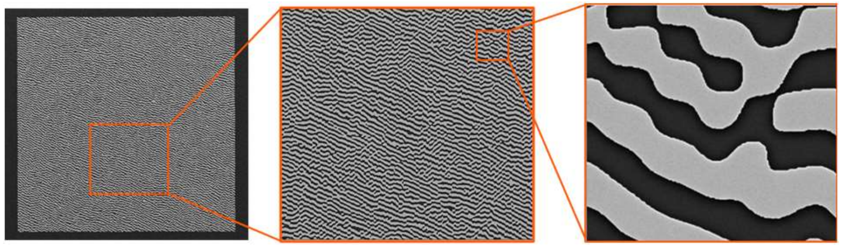

References

[1] E. Albisetti et al., Comm. Phys., 1 (56) **2018**.

[2] E. Albisetti et al., *Nat. Nanotechnol. 11 (545)* **2016**.

[3] E. Albisetti et al., *Appl. Phys. Lett. 113 (162401)* **2018**.

[4] E. Albisetti et al., *AIP Adv. 7 (055601)* **2017**.

[5] E. Albisetti et al., *J. Magn. Magn. Mater. 400 (230)* **2016**.

[6] E. Albisetti et al., Adv. Mater. (1906439) **2020**.

[7] Rawlings et al., *Nanotechnology*, 29 (505302) **2018**.

[8] Skaug et al., Science, 359 (1505) **2018**.

[9] Zheng *et al.*, *Nat. Electron.*, 2 (17) **2019**.